

Kinematic Modularity of Elementary Dynamic Actions

Moses C. Nah,¹ Johannes Lachner,¹ Federico Tessari,¹ and Neville Hogan^{1,2}

Abstract—In this paper, a kinematically modular approach to robot control is presented. The method involves structures called Elementary Dynamic Actions and a network model combining these elements. With this control framework, a rich repertoire of movements can be generated by combination of basic kinematic modules. Each module can be learned by Imitation Learning, thereby resulting in a modular learning strategy for robot control. The theoretical foundations and their real robot implementation are presented. Using a KUKA LBR iiwa14 robot, three tasks were considered: (1) generating a sequence of discrete movements, (2) generating a combination of discrete and rhythmic movements, and (3) a drawing and erasing task. The obtained results indicate that this modular approach has the potential to simplify the generation of a diverse range of robot actions.

I. INTRODUCTION

To generate complex motor behavior that can match that of humans, robot control based on motor primitives has been proposed [1]–[11]. The method originates from motor neuroscience research, where the complex motor behavior of biological systems appears to be generated by a combination of fundamental building blocks [12]–[19]. By parameterizing a controller using motor primitives, robots can efficiently learn, adapt, and execute a wide range of tasks.

In robotics, two distinct motor-primitive approaches have been identified: Elementary Dynamic Actions (EDA)* [8]–[10] and Dynamic Movement Primitives (DMP) [6], [20]. EDA provides a modular framework for robot control that also accounts for physical interaction [8]–[11], [21]. One of its applications, impedance control [22]–[24], has been a prominent approach for tasks involving contact and physical interaction. DMP provides a rigorous mathematical framework to generate movements of arbitrary complexity [6], [20]. Its prominent application, Imitation Learning (or Learning from Demonstration [4], [5]), provides a systematic method to learn (or imitate) trajectories that are provided by demonstration.

In this paper, we combine EDA with DMP to achieve a modular learning approach for robot control. Using this

control framework, a wide range of robot movements can be produced by combining basic modules. Each module can be learned with Imitation Learning, resulting in “modular” Imitation Learning. This approach also preserves the advantages of EDA for tasks involving contact and physical interaction.

A theoretical overview of the proposed modular strategy is presented, together with an actual robot implementation. Using a KUKA LBR iiwa14 robot, a modular control in task-space is demonstrated. Three tasks are considered: (1) generating a sequence of discrete movements, (2) generating a combination of discrete and rhythmic movements, (3) a drawing and erasing task. The first two tasks highlight the kinematic modularity offered by EDA; the third task serves as an illustrative example of combining the modular property of EDA with DMP’s Imitation Learning. These demonstrations show the proposed approach has the potential to simplify the generation of a range of diverse robot motions.

II. THEORETICAL FOUNDATIONS

In this section, a brief overview of EDA and DMP is provided. A torque-actuated n degrees of freedom (DOFs) open-chain robotic manipulator is considered.

A. Elementary Dynamic Actions and the Norton Equivalent Network Model

EDA, introduced by Hogan and Sternad [8]–[10], consist of (at least) three distinct classes of primitives (Figure 1A):

- Submovements for discrete movements [25].
- Oscillations for rhythmic movements [25].
- Mechanical impedances to manage physical interaction [11].

This paper will focus on submovements and oscillations. Only the necessary details of mechanical impedances are briefly presented.

1) *Kinematic Primitives — Submovements and Oscillations*: A submovement $\mathbf{x}_0 : \mathbb{R}_{\geq 0} \rightarrow \mathbb{R}^n$ is a smooth trajectory with a time derivative that is a unimodal function, i.e., has a single peak value:

$$\dot{\mathbf{x}}_0(t) = \mathbf{v} \hat{\sigma}(t) \quad (1)$$

In this equation, $t \in \mathbb{R}_{\geq 0}$ is time; $\hat{\sigma} : \mathbb{R}_{\geq 0} \rightarrow [0, 1]$ denotes a smooth unimodal basis function with peak value 1; $\mathbf{v} \in \mathbb{R}^n$ is the velocity amplitude of each DOF. Since submovements model discrete movement, $\hat{\sigma}(t)$ has a finite support, i.e., there exists $T > 0$ such that $\hat{\sigma}(t) = 0$ for $t \geq T$.

An oscillation $\mathbf{x}_0 : \mathbb{R}_{\geq 0} \rightarrow \mathbb{R}^n$ is a smooth non-zero trajectory which is a periodic function:

$$\forall t > 0 : \exists T > 0 : \mathbf{x}_0(t) = \mathbf{x}_0(t+T) \quad (2)$$

¹Department of Mechanical Engineering, Massachusetts Institute of Technology, Cambridge, MA, USA.

²Department of Brain and Cognitive Sciences, Massachusetts Institute of Technology, Cambridge, MA, USA.

This work was supported in part by the MIT/SUSTech Centers for Mechanical Engineering Research and Education. MCN was supported in part by a Mathworks Fellowship.

This work has been submitted to the IEEE for possible publication. Copyright may be transferred without notice, after which this version may no longer be accessible.

*The original name suggested by Hogan and Sternad [8] was “Dynamic Motor Primitives.” However, to avoid confusion due to the similarity to “Dynamic Movement Primitives,” we instead use “Elementary Dynamic Actions.”

Compared to submovements, oscillations model rhythmic and repetitive motions.

2) *Interactive Primitive — Mechanical Impedances*: Mechanical impedance $\mathbf{Z} : \mathbb{R}^n \rightarrow \mathbb{R}^n$ is an operator which maps (generalized) displacement $\Delta \mathbf{x}(t) \in \mathbb{R}^n$ to (generalized) force $\mathbf{F}(t) \in \mathbb{R}^n$ [10], [11], [21]:

$$\mathbf{Z} : \Delta \mathbf{x}(t) \longrightarrow \mathbf{F}(t)$$

In this equation, $\Delta \mathbf{x}(t)$ is the displacement of an actual trajectory of (generalized) position $\mathbf{x}(t)$ from a virtual trajectory $\mathbf{x}_0(t)$ to which the mechanical impedance is connected, i.e., $\Delta \mathbf{x}(t) = \mathbf{x}_0(t) - \mathbf{x}(t)$. Loosely speaking, mechanical impedance is a generalization of stiffness to encompass nonlinear dynamic behavior [10].

Mechanical impedances can be linearly superimposed even though each mechanical impedance is a nonlinear operator. This is the superposition principle of mechanical impedances [10], [11], [21], [23]:

$$\mathbf{Z} = \sum \mathbf{Z}_i \quad (3)$$

Note that the impedance operators can include transformation maps (i.e., Jacobian matrices) (Section III).

While mechanical impedance introduces favorable properties which simplify a wide range of control tasks, in this paper we will focus on kinematic primitives of EDA, i.e., submovements and oscillations. For more details on the use of mechanical impedance, readers are referred to [10], [21], [26]–[29].

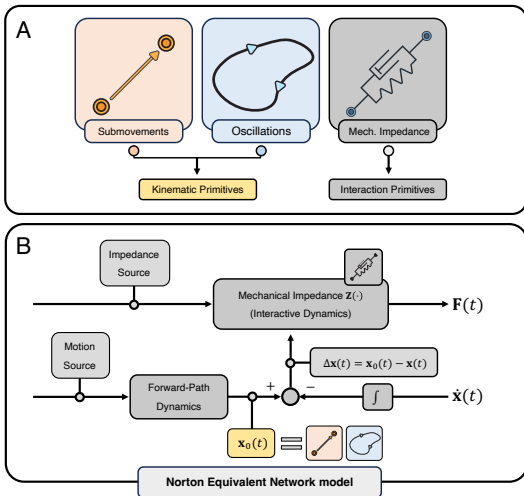


Fig. 1. (A) Three Elementary Dynamic Actions (EDA). Submovements (orange box) and oscillations (blue box) correspond to kinematic primitives and mechanical impedances manage physical interaction. (B) EDA combined using a Norton equivalent network model. The virtual trajectory $\mathbf{x}_0(t)$ (yellow box) consists of submovements (orange box) and/or oscillations (blue box), and mechanical impedance \mathbf{Z} regulates interactive dynamics.

3) *Norton Equivalent Network Model*: The three distinct classes of EDA can be combined using a Norton equivalent network model [10], which provides an effective framework to relate the three classes of EDA (Figure 1B). The forward-path dynamics specifies the virtual trajectory $\mathbf{x}_0(t)$, which

consists of submovements and/or oscillations. The mechanical impedance \mathbf{Z} , determines $\mathbf{F}(t)$ with the virtual trajectory $\mathbf{x}_0(t)$, and its (generalized) force output $\mathbf{F}(t)$ is used as an input to the robot. Hence, a key objective of EDA is to find appropriate choices of $\mathbf{x}_0(t)$ and \mathbf{Z} to generate the desired robot behavior.

By combining EDA with the Norton equivalent network model, submovements and/or oscillations can be directly superimposed at the level of the virtual trajectory $\mathbf{x}_0(t)$. This is the core concept that provides kinematic modularity of EDA, which simplifies generating a wide range of movements (Section III).

B. Dynamic Movement Primitives and Imitation Learning

DMP, introduced by Ijspeert, Schaal, et al. [6] consists of three distinct classes of primitives: canonical system, nonlinear forcing term and transformation system. Using these three primitives, DMP can represent both discrete and rhythmic movements. However, different choices of canonical systems and nonlinear forcing terms are employed for these movements [6]. For this overview, we focus on DMP for discrete movement.

1) *Dynamic Movement Primitives*: A canonical system for discrete movement $s : \mathbb{R}_{\geq 0} \rightarrow \mathbb{R}_{\geq 0}$ is a scalar variable governed by a stable first-order differential equation:

$$\tau \dot{s}(t) = -\alpha_s s(t)$$

In this equation, α_s and τ are positive constants.

A nonlinear forcing term for discrete movement, $f : \mathbb{R}_{\geq 0} \rightarrow \mathbb{R}$, which takes the canonical system $s(t)$ as the function argument, is defined by:

$$f(s(t)) = \frac{\sum_{i=1}^N w_i \phi_i(s(t))}{\sum_{i=1}^N \phi_i(s(t))} s(t) (g - y_0) \quad (4)$$

$$\phi_i(s(t)) = \exp \left\{ -h_i (s(t) - c_i)^2 \right\}$$

In these equations, $\phi_i : \mathbb{R}_{\geq 0} \rightarrow \mathbb{R}_{\geq 0}$ is the i -th basis function of the nonlinear forcing term which is a Gaussian function; N is the number of basis functions; y_0 and g are the initial and final positions of the discrete movement, respectively; w_i is the weight and c_i, h_i determine the center, width of the i -th basis function, respectively.

A transformation system is a second-order differential equation with a nonlinear forcing term $f(s(t))$ as an input:

$$\tau_y \dot{y}(t) = z(t)$$

$$\tau_z \dot{z}(t) = \alpha_z \{ \beta_z (g - y(t)) - z(t) \} + f(s(t)) \quad (5)$$

In these equations, α_z and β_z are positive constants; $y(t)$ and $z(t)$ are state variables which correspond to position and (time-scaled) velocity of the transformation system, respectively. $y(t)$ can represent both joint-space and task-space trajectories. However, for end-effector orientation, a different transformation system must be employed [30], [31].

2) *Imitation Learning*: Imitation Learning generates (or mimics) a desired trajectory $y_{des}(t)$ by learning the best-fit weights of the nonlinear forcing term $f(s(t))$ (Eq. (4)). Given P sample points of $(y_{des}(t_j), \dot{y}_{des}(t_j), \ddot{y}_{des}(t_j))$ for $j \in [1, 2, \dots, P]$, the best-fit weight w_i^* is calculated using Locally Weighted Regression [6], [32], [33]:

$$w_i^* = \frac{\sum_{j=1}^P a_j \phi_{ij} f_j}{\sum_{j=1}^P a_j^2 \phi_{ij}} \quad (6)$$

$$a_j = s(t_j)(g - y_0) \quad \phi_{ij} = \phi_i(s(t_j))$$

$$f_j = \tau^2 \ddot{y}_{des}(t_j) + \alpha_z \tau \dot{y}_{des}(t_j) + \alpha_z \beta_z \{y_{des}(t_j) - g\}$$

Along with Locally Weighted Regression, one can also use Linear Least Square Regression to find the best-fit weights [30], [31]. To use Imitation Learning for $y_{des}(t)$, one must also calculate the velocity $\dot{y}_{des}(t)$ and acceleration $\ddot{y}_{des}(t)$.

To generalize Imitation Learning to an n -DOF system, n transformation systems with n nonlinear forcing terms may be synchronized with a single canonical system [6]. For a desired trajectory $\mathbf{y}_{des}(t) \in \mathbb{R}^n$, Imitation Learning for each DOF is conducted [30], [31], [34]–[37].

III. THE THREE CONTROL TASKS AND METHODS

In this section, we introduce three control tasks and the corresponding methods to achieve them.

- 1) Generating a sequence of discrete movements.
- 2) Generating a combination of discrete and rhythmic movements.
- 3) Drawing and erasing a path on a table.

The first two tasks highlight the advantages of EDA's kinematic modularity. The final task, which involves physical contact, provides an illustrative example of how Imitation Learning can be combined with EDA.

The torque command of a robot, $\boldsymbol{\tau}_{in}(t) \in \mathbb{R}^n$ is defined by superimposing three mechanical impedances (Eq. (3)):

$$\boldsymbol{\tau}_{in}(t) = \mathbf{Z}_q(\mathbf{q}) + \mathbf{J}_p(\mathbf{q})^T \mathbf{Z}_p(\mathbf{p}, \mathbf{p}_0(t)) + \mathbf{J}_r(\mathbf{q})^T \mathbf{Z}_r(\mathbf{R}, \mathbf{R}_0) \quad (7)$$

where:

$$\begin{aligned} \mathbf{Z}_q(\mathbf{q}) &= -\mathbf{B}_q \dot{\mathbf{q}} \\ \mathbf{Z}_p(\mathbf{p}, \mathbf{p}_0(t)) &= \mathbf{K}_p \{\mathbf{p}_0(t) - \mathbf{p}\} + \mathbf{B}_p \{\dot{\mathbf{p}}_0(t) - \dot{\mathbf{p}}\} \\ \mathbf{Z}_r(\mathbf{R}, \mathbf{R}_0) &= k_r \mathbf{R} \mathbf{Log}(\mathbf{R}^T \mathbf{R}_0) - b_r \boldsymbol{\omega} \end{aligned} \quad (8)$$

In these equations, $\mathbf{q} \equiv \mathbf{q}(t) \in \mathbb{R}^n$ denotes the robot's joint trajectories; $\mathbf{p} \equiv \mathbf{p}(\mathbf{q}(t)) \in \mathbb{R}^3$ and $\mathbf{R} \equiv \mathbf{R}(\mathbf{q}(t)) \in \text{SO}(3)$ are the robot's end-effector position and orientation, respectively; \mathbf{p} and \mathbf{R} are derived by the Forward Kinematics Map of the robot; $\mathbf{J}_p(\mathbf{q}), \mathbf{J}_r(\mathbf{q}) \in \mathbb{R}^{3 \times n}$ denote the Jacobian matrices for the translational velocity $\dot{\mathbf{p}}$ and rotational velocity $\boldsymbol{\omega}$ of the end-effector, respectively, i.e., $\dot{\mathbf{p}} = \mathbf{J}_p(\mathbf{q})\dot{\mathbf{q}}$ and $\boldsymbol{\omega} = \mathbf{J}_r(\mathbf{q})\dot{\mathbf{q}}$; $\mathbf{R}_0 \in \text{SO}(3)$ denotes the virtual end-effector orientation which is set to be constant; $\mathbf{Log} : \text{SO}(3) \rightarrow \mathbb{R}^3$ denotes the Matrix Logarithm Map. For more details about Special Orthogonal Group $\text{SO}(3)$ and the Matrix Logarithmic Map, readers are referred to [38], [39].

$\mathbf{Z}_q, \mathbf{Z}_p, \mathbf{Z}_r$ correspond to joint-space impedance, translational task-space impedance, and rotational task-space

impedance, respectively; $\mathbf{B}_q \in \mathbb{R}^{n \times n}$ denotes the joint damping matrix; $\mathbf{K}_p, \mathbf{B}_p \in \mathbb{R}^{3 \times 3}$ denote the translational stiffness and damping matrices, respectively; $k_r, b_r \in \mathbb{R}$ denote the rotational stiffness and damping coefficients, respectively; Matrices $\mathbf{K}_q, \mathbf{K}_p, \mathbf{B}_p$ (respectively k_r, b_r) are chosen to be constant symmetric positive definite matrices (respectively positive values).

The virtual end-effector trajectory is denoted $\mathbf{p}_0(t) \in \mathbb{R}^3$, which consists of submovements and/or oscillations (Section II-A). Hence, with the impedance parameters $\mathbf{Z}_q, \mathbf{Z}_p$, and \mathbf{Z}_r set to be constant, the control objective is to define trajectory $\mathbf{p}_0(t)$ that achieves the three control tasks.

A. Generating a Sequence of Discrete Movements

Given an initial end-effector position $\mathbf{p}_1 \in \mathbb{R}^3$, let $\mathbf{p}_2 \in \mathbb{R}^3$ be a goal location which the robot's end-effector aims to reach. This goal-directed discrete movement $\mathbf{p}(t) \rightarrow \mathbf{p}_2$ can be achieved by setting $\mathbf{p}_0(t)$ as $\mathbf{p}_{0,sub1}(t)$ [40]–[43]:

$$\mathbf{p}_{0,sub1}(t) = \begin{cases} \mathbf{p}_1 & 0 \leq t < t_i \\ \mathbf{p}_1 + (\mathbf{p}_2 - \mathbf{p}_1)f_1(t) & t_i \leq t < t_i + T_1 \\ \mathbf{p}_2 & t_i + T_1 \leq t \end{cases} \quad (9)$$

In these equations, $f_1(t)$ is a submovement starting at time t_i with duration T_1 (Eq. (1))

At time t_g , the goal location suddenly changes to a new goal location $\mathbf{p}_3 \in \mathbb{R}^3$, which necessitates a second movement. Using the kinematic modularity of EDA, the end-effector can reach \mathbf{p}_3 by superimposing another submovement $\mathbf{p}_{0,sub2}(t)$, without modifying $\mathbf{p}_{0,sub1}(t)$:

$$\begin{aligned} \mathbf{p}_0(t) &= \mathbf{p}_{0,sub1}(t) + \mathbf{p}_{0,sub2}(t) \\ \mathbf{p}_{0,sub2}(t) &= \begin{cases} \mathbf{0} & 0 \leq t < t_g \\ (\mathbf{p}_3 - \mathbf{p}_2)f_2(t) & t_g \leq t < t_g + T_2 \\ \mathbf{p}_3 & t_g + T_2 \leq t \end{cases} \end{aligned} \quad (10)$$

In these equations, $f_2(t)$ is a submovement starting at time t_g with duration T_2 . With this new $\mathbf{p}_0(t)$ combined with the two submovements $\mathbf{p}_{0,sub1}(t)$ and $\mathbf{p}_{0,sub2}(t)$, the convergence of $\mathbf{p}(t)$ to the new goal \mathbf{p}_3 is achieved [40]–[43].

B. Generating a Combination of Discrete and Rhythmic Movements

Consider a goal-directed discrete movement from starting location $\mathbf{p}_1 \in \mathbb{R}^3$ to goal location $\mathbf{p}_2 \in \mathbb{R}^3$. As discussed in Section III-A, this movement can be achieved by a single submovement $\mathbf{p}_{0,sub1}(t)$, i.e., (Eq. (9)). Our goal is to overlap a rhythmic movement onto this goal-directed discrete movement. This can be achieved by direct summation of an oscillation $\mathbf{p}_{0,osc}(t)$ (Eq. (2)) onto $\mathbf{p}_{0,sub1}(t)$:

$$\mathbf{p}_0(t) = \mathbf{p}_{0,osc}(t) + \mathbf{p}_{0,sub1}(t) \quad (11)$$

C. Drawing and Erasing Task

Consider a task of teaching a robot to draw trajectory $\mathbf{p}_{des}(t) \in \mathbb{R}^2$ on a table. Without loss of generality, assume that the drawing table resides on a horizontal XY -plane. After drawing $\mathbf{p}_{des}(t)$, the robot retraces $\mathbf{p}_{des}(t)$ with an additional oscillatory movement to thoroughly erase the trajectory.

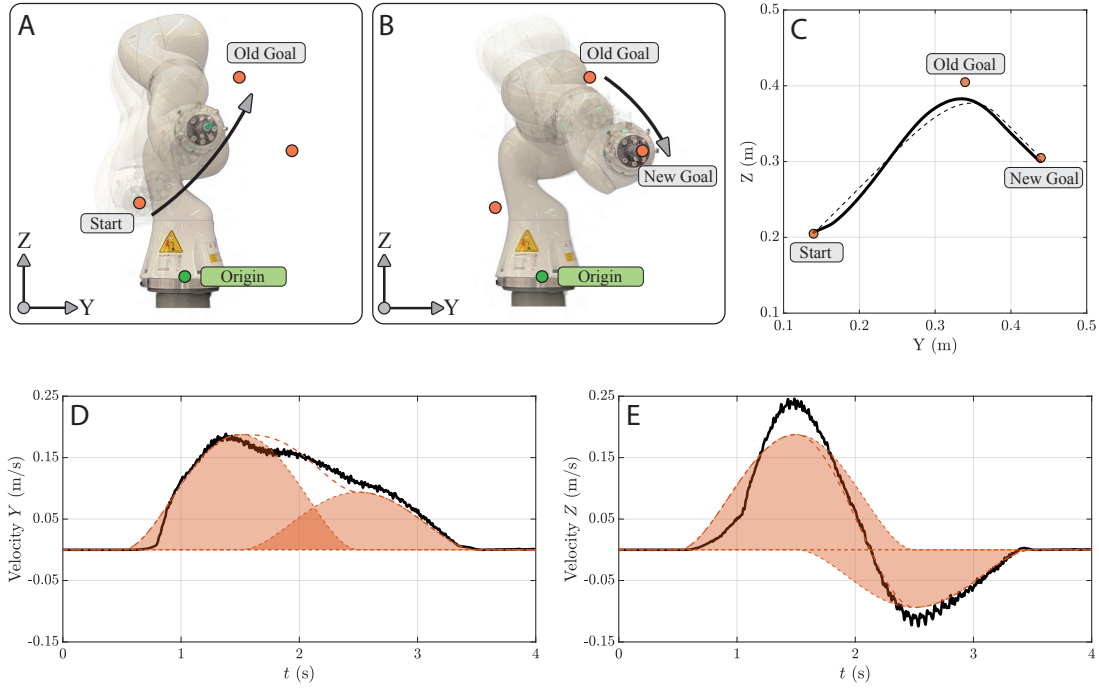


Fig. 2. A sequence of discrete movements using a KUKA LBR iiwa14. (A, B) Time-lapse of the robot movement towards the (A) original (old) and (B) new goal location. Start \mathbf{p}_1 , original goal \mathbf{p}_2 and new goal \mathbf{p}_3 are depicted as orange markers. The origin of the robot’s coordinate frame is attached at the robot base, depicted as a green marker. (C) The end-effector trajectory $\mathbf{p}(t)$ (black filled line) and the virtual trajectory (black dashed line) $\mathbf{p}_0(t)$ depicted on the YZ -plane. (D, E) Time t vs. end-effector velocity $\dot{\mathbf{p}}(t)$ along the (D) Y -coordinate and (E) Z -coordinate. Black filled lines show the end-effector velocity, which was derived by a first-order finite difference of $\mathbf{p}(t)$ with a sampling interval of 3ms. The two unimodal speed profiles filled in orange depict the two submovements $\mathbf{p}_{0,sub1}(t)$ (left) (Eq. (9)) and $\mathbf{p}_{0,sub2}(t)$ (right) (Eq. (10), (13)). As shown in (D) and (E), the second submovement is directly superimposed, without any modification of the first submovement. Parameters of the submovements (Eq. (9), (10), (13)): $\mathbf{p}_1 = [0.6735, 0.1396, 0.2048]m$, $\mathbf{p}_2 = [0.6735, 0.3396, 0.4048]m$, $\mathbf{p}_3 = [0.6735, 0.4396, 0.3048]m$, $T_1 = 2.0s$, $T_2 = 2.0s$, $t_i = 0.5s$, $t_g = 1.5s$.

For this drawing and erasing task, one can combine Imitation Learning with EDA. In detail, Imitation Learning with a two-dimensional DMP was used to learn $\mathbf{p}_{des}(t)$ and this trajectory was used as the X - and Y -coordinates of $\mathbf{p}_0(t)$ to draw $\mathbf{p}_{des}(t)$.

Once $\mathbf{p}_{des}(t)$ is drawn on the plane, the drawing can be erased by simply superimposing an oscillation $\mathbf{p}_{0,osc}(t)$ on a time-reversed trajectory of $\mathbf{p}_{des}(t)$:

$$\mathbf{p}_0(t) = \begin{cases} \mathbf{p}_{des}(T-t) + \mathbf{p}_{0,osc}(t) & 0 \leq t < T \\ \mathbf{p}_{0,osc}(t) & T \leq t \end{cases} \quad (12)$$

In this equation, $T \in \mathbb{R}_{>0}$ is the duration of $\mathbf{p}_{des}(t)$.

Note that the Z -coordinates of $\mathbf{p}_0(t)$, $p_{0,z}(t)$, is not learned with Imitation Learning. Instead, an appropriate value of $p_{0,z}(t)$ must be chosen to remain in contact with the table. To elaborate, let the Z -coordinate of the drawing table be h_z . The pen extended from the robot’s end-effector is facing downward, towards the $-Z$ direction. To ensure that the pen maintains contact with the plane throughout its operation, it is necessary to set $p_{0,z}(t)$ lower than the drawing plane h_z with an offset $\varepsilon > 0$, i.e., $p_{0,z}(t) = h_z - \varepsilon$. Moreover, since $\boldsymbol{\tau}_{in}(t)$ includes \mathbf{Z}_r with constant \mathbf{R}_0 , the drawing can be achieved while maintaining orientation [44], [45].

IV. EXPERIMENTAL RESULTS

For the robot experiment, we use KUKA LBR iiwa14, which has seven torque-actuated DOFs (i.e., $n = 7$). For

control, KUKA’s Fast Robot Interface (FRI) was employed. For all three tasks, the built-in gravity compensation was activated. For the impedance parameters \mathbf{B}_q , k_r and b_r (Eq. (8)), identical values were used for all three tasks. The impedance values: $\mathbf{B}_q = 1.0\mathbf{I}_7 \text{ N} \cdot \text{m} \cdot \text{s}/\text{rad}$, where $\mathbf{I}_n \in \mathbb{R}^{n \times n}$ denotes an identity matrix; $k_r = 50 \text{ N} \cdot \text{m}/\text{rad}$, $b_r = 5 \text{ N} \cdot \text{m} \cdot \text{s}/\text{rad}$. $\mathbf{q}(t)$ was directly called from the FRI interface; $\dot{\mathbf{q}}(t)$ was derived by first-order finite difference of $\mathbf{q}(t)$ with a time step of 3ms. The Forward Kinematics Map to derive \mathbf{p} , \mathbf{R} , and the Jacobian matrices $\mathbf{J}_p(\mathbf{q})$, $\mathbf{J}_r(\mathbf{q})$ were calculated using Exp[licit]TM-FRI Library.[†]

A. Generating a Sequence of Discrete Movements

For the basis function of the two submovements $\mathbf{p}_{0,sub1}(t)$ (Eq. (9)) and $\mathbf{p}_{0,sub2}(t)$ (Eq. (10)), a minimum-jerk trajectory was used [46]:

$$\begin{aligned} f_1(t) &= 10 \left(\frac{t-t_i}{T_1} \right)^3 - 15 \left(\frac{t-t_i}{T_1} \right)^4 + 6 \left(\frac{t-t_i}{T_1} \right)^5 \\ f_2(t) &= 10 \left(\frac{t-t_g}{T_2} \right)^3 - 15 \left(\frac{t-t_g}{T_2} \right)^4 + 6 \left(\frac{t-t_g}{T_2} \right)^5 \end{aligned} \quad (13)$$

The values of the impedance parameters \mathbf{K}_p , \mathbf{B}_p (Eq. (8)) were $800\mathbf{I}_3 \text{ N}/\text{m}$, $80\mathbf{I}_3 \text{ N} \cdot \text{s}/\text{m}$, respectively.

The results are shown in Figure 2. With the proposed approach, a convergence of $\mathbf{p}(t)$ to the new goal location \mathbf{p}_3

[†] Github repository: <https://github.com/explicit-robotics/Explicit-FRI>

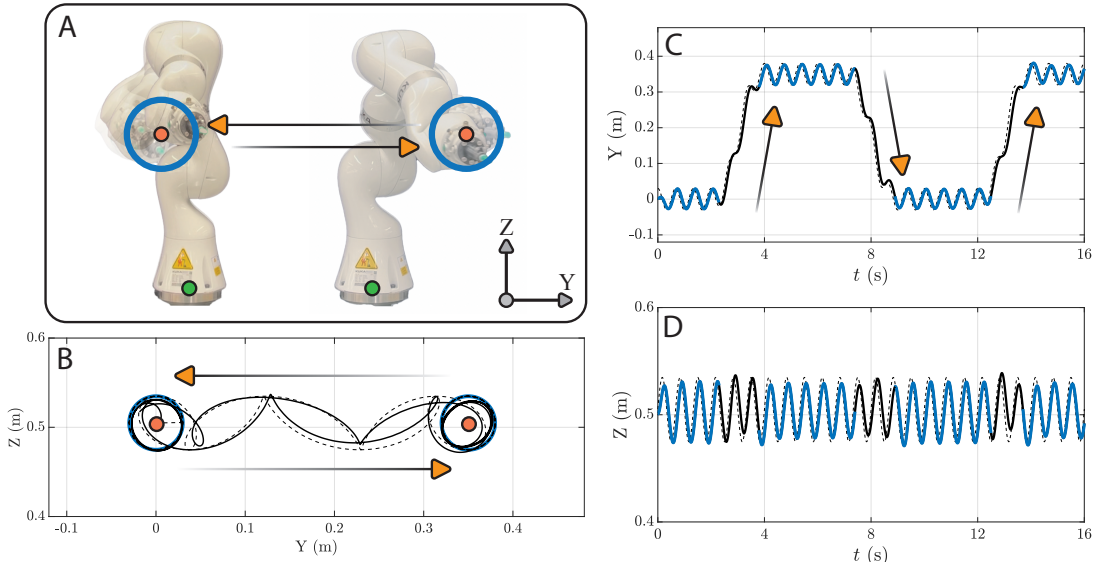


Fig. 3. A combination of discrete and rhythmic movements using a KUKA LBR iiwa14. (A) Elements of the robot movement. The origin of the robot's coordinate frame is attached at the robot base, depicted as green marker. Orange markers depict \mathbf{p}_1 (left) and \mathbf{p}_2 (right) of $\mathbf{p}_{0,sub1}(t)$. Blue line depicts $\mathbf{p}_{0,osc}(t)$ (Eq. (11), (14)). (B) The end-effector trajectory $\mathbf{p}(t)$ (black filled line) and the virtual trajectory (black dashed line) $\mathbf{p}_0(t)$ depicted on the YZ -plane. Multiple submovements that move between \mathbf{p}_1 and \mathbf{p}_2 were generated. (C, D) Time t vs. end-effector trajectory $\mathbf{p}(t)$ along (C) Y -coordinate and (D) Z -coordinate. Black dashed lines depict $\mathbf{p}_0(t)$. Blue lines highlight the duration of a movement without any discrete movement. Parameters of submovement and oscillation (Eq. (11), (14)): $\mathbf{p}_1 = [0.5735, 0.0, 0.5048]m$, $\mathbf{p}_2 = [0.5735, 0.35, 0.5048]m$, $T_1 = 1.5s$, $r = 0.03m$, $\omega_0 = 3\pi rad/s$.

was achieved (Figure 2A, 2B) by simply superimposing a second submovement onto the first one (Figure 2C, 2D, 2E). It is worth emphasizing that the task was achieved without any modification of the first submovement. The simplicity of this approach is not guaranteed for other methods. For instance, using DMP, the task requires online modification of the initiated movement [47], which may introduce practical difficulties for implementation (Eq. (5)).

B. Generating a Combination of Discrete and Rhythmic Movements

For the submovement, $\mathbf{p}_{0,sub1}(t)$ was employed. For the oscillation, a circular trajectory residing on the YZ -plane was used:

$$\mathbf{p}_{0,osc}(t) = r[0, \cos(\omega_0 t), \sin(\omega_0 t)] \quad (14)$$

In this equation, r and ω_0 are the radius and angular velocity of the circular trajectory, respectively. The values of the impedance parameters were identical to those in Section IV-A, i.e., $\mathbf{K}_p = 800\mathbf{I}_3 N/m$ and $80\mathbf{I}_3 N \cdot s/m$, respectively (Eq. (8)). The results are shown in Figure 3. With the proposed approach, a combination of discrete and rhythmic movements of the robot's end-effector was achieved (Figure 3A) by simply superimposing submovement and oscillation (Figure 3B, 3C, 3D). Note that this direct combination of both discrete and rhythmic movements may not be obvious for DMP, since DMP accounts for these two movements separately [6], [48]–[50] (Section II-B).

C. Drawing and Erasing Task

For Imitation Learning of $\mathbf{p}_{des}(t)$, the human-demonstrated data points of $\mathbf{p}_{des}(t)$ were collected with a sampling rate of

333Hz. The velocity $\dot{\mathbf{p}}_{des}(t)$ and acceleration $\ddot{\mathbf{p}}_{des}(t)$ for Imitation Learning were derived by first-order finite difference of $\mathbf{p}_{des}(t)$ with Gaussian filtering. For the filtering, MATLAB's `smoothdata` function with a time window size 165ms was used. With these filtered data, Locally Weighted Regression was used for Imitation Learning (Eq. (6)). For the drawing (respectively erasing), the impedance parameters \mathbf{K}_p and \mathbf{B}_p were chosen to be $400\mathbf{I}_3 N/m$ (respectively $800\mathbf{I}_3 N/m$) and $40\mathbf{I}_3 N \cdot s/m$ (respectively $80\mathbf{I}_3 N \cdot s/m$). For the erasing, an oscillation $\mathbf{p}_{0,osc}(t)$ of Eq. (14) but residing on the XY -plane (not the YZ -plane) was used.

The results are shown in Figure 4, which shows the whole process of generating $\mathbf{p}_0(t)$ for the drawing and erasing tasks. By merging Imitation Learning with EDA (Figure 4A, 4B, 4C), the drawing (Figure 4D) and erasing tasks (Figure 4E) were successfully achieved. It is worth emphasizing that the key to this approach is the combination of Imitation Learning and the modular property of EDA. The trajectory $\mathbf{q}_{des}(t)$ was separately learned with Imitation Learning and directly combined with an oscillation $\mathbf{p}_{0,osc}(t)$. With modest parameter tuning (i.e., changing the angular velocity ω_0), trajectory $\mathbf{p}_{0,osc}(t)$ used in task IV-B was simply reused.

V. DISCUSSION AND CONCLUSION

Thanks to the kinematic modularity of EDA, the two tasks of (1) sequencing discrete movements and (2) combining discrete and rhythmic movements were greatly simplified. For the former, the subsequent movement was directly superimposed onto the previous movement, without any modification of the first submovement. For the latter, the discrete and rhythmic movements were separately planned and directly superimposed. The authors want to emphasize that the sim-

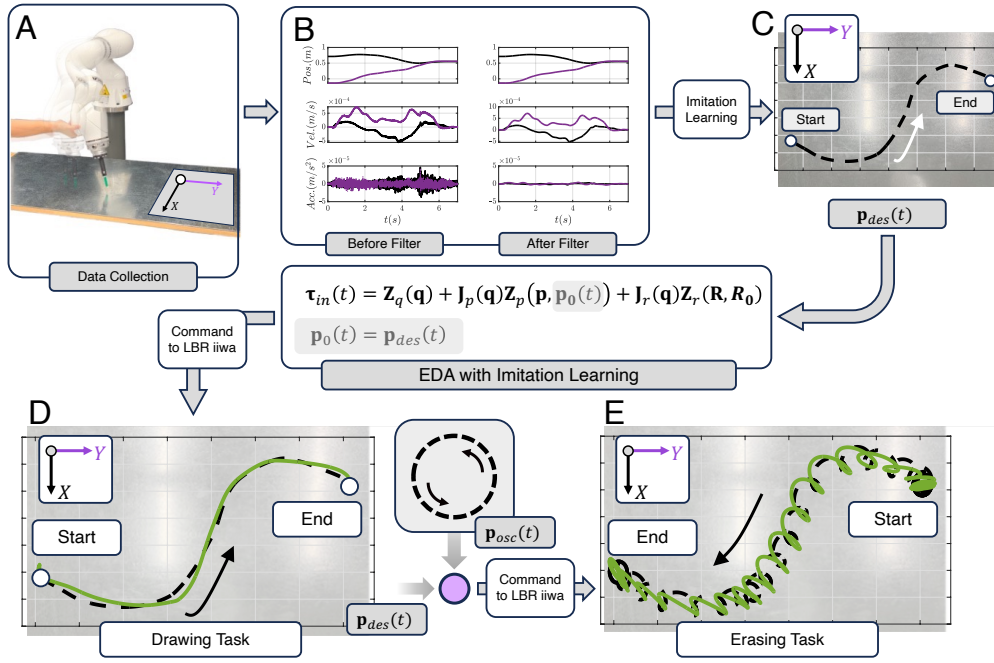


Fig. 4. The drawing and erasing task using a KUKA LBR iiwa. A green pen was used for the drawing. (A) Data collection of human-demonstrated $\mathbf{p}_{des}(t)$ which we aim to draw (Section III-C). The end-effector trajectory along X - and Y -coordinates were collected. (B) Time t vs. X -coordinate (black line) and Y -coordinate (purple line) of $\mathbf{p}_{des}(t)$ (top row), $\dot{\mathbf{p}}_{des}(t)$ (middle row), $\ddot{\mathbf{p}}_{des}(t)$ (bottom row). With a sampling rate of 333Hz, a first-order finite difference method was used to calculate the velocity and acceleration (left column). These trajectories were Gaussian filtered (right column) using MATLAB's `smoothdata` function with a time window size of 165ms. (C) The resulting trajectory $\mathbf{p}_{des}(t)$ (black dashed line) generated with Imitation learning. (D) The drawing task was achieved by setting $\mathbf{p}_0(t)$ as $\mathbf{p}_{des}(t)$. The black dashed line depicts $\mathbf{p}_0(t)$ (or $\mathbf{p}_{des}(t)$), green line depicts $\mathbf{p}(t)$. (E) The erasing task was achieved by superimposing an oscillation $\mathbf{p}_{osc}(t)$ onto a time-reversed $\mathbf{p}_{des}(t)$. The green line depicts $\mathbf{p}(t)$. For (C, D, E), trajectories were plotted in MATLAB and overlapped onto the drawing/erasing table. Parameters of DMP: $\alpha_c = 1000$, $\beta_c = 250$, $N = 100$, $P = 2331$, $\tau = 7$, $c_i = \exp(-\alpha_c(i-1)/(N-1))$, $h_i = 1/(c_{i+1} - c_i)^2$ for $i \in [1, 2, \dots, N-1]$, $c_N = \exp(-\alpha_c)$, $h_N = h_{N-1}$. Parameters of oscillation: $r = 0.03m$, $\omega_0 = 2\pi rad/s$.

plicity of this approach is not trivial. For example, using DMP, the former task is achieved by using an additional online modulation method, or by introducing an additional dynamics for goal g . These additional methods may pose practical challenges for actual robot implementation. For the latter task, DMP accounts for discrete and rhythmic movements separately [6], [48]–[50]. Hence, one cannot directly combine the two movements generated (or learned) by DMP.

The robot demonstration of the drawing and erasing task illustrated how to get the best of both motor-primitives approaches. DMP and Imitation Learning provided a rigorous mathematical framework to generate (or learn) trajectories of arbitrary complexity. EDA and its Norton equivalent network model provided a modular framework for robot control. Using Imitation Learning to learn the virtual trajectory of EDA, a modular learning strategy for robot control was established. While the presented example focused on modular control of end-effector position, the approach can be generalized to different coordinates. For instance, Imitation Learning of end-effector orientation and end-effector position can be separately conducted and later combined using the modular property of EDA.

Merging the methods of EDA with DMP preserved the kinematic modularity of EDA and combined it with its favor-

able behavior during physical interaction. This facilitated the drawing and erasing task, which involves physical contact. The key to this approach is the compliant robot behavior emerging from mechanical impedances, which may be challenging to generate using position-actuated robots [21]. However, the compliance of mechanical impedances resulted in non-negligible tracking error between the virtual and actual end-effector trajectory. This might be ameliorated to some degree by increasing impedance in the direction of desired motion. Nonetheless, the authors consider that the modular approach presented using torque-actuated robots, outweighs the advantages of utilizing position-actuated robots.

As discussed, a key objective of EDA is to find appropriate choices of virtual trajectory and the corresponding mechanical impedance. The former property was addressed in this paper by using the Imitation Learning of DMP, which thereby resulted in modular Imitation Learning. However, choosing appropriate values of mechanical impedance may not be obvious; the presented values were discovered by trial-and-error. A systematic method to choose (or learn) the impedance parameters is an avenue of future research [51].

In conclusion, by integrating EDA with DMP's Imitation Learning, a modular learning strategy for robot control was established. This modular approach has great potential to simplify the generation of a wide range of robot actions.

REFERENCES

- [1] S. Schaal, "Learning from demonstration," *Advances in neural information processing systems*, vol. 9, 1996.
- [2] —, "Is imitation learning the route to humanoid robots?" *Trends in cognitive sciences*, vol. 3, no. 6, pp. 233–242, 1999.
- [3] A. J. Ijspeert, J. Nakanishi, and S. Schaal, "Movement imitation with nonlinear dynamical systems in humanoid robots," in *Proceedings 2002 IEEE International Conference on Robotics and Automation (Cat. No. 02CH37292)*, vol. 2. IEEE, 2002, pp. 1398–1403.
- [4] S. Calinon and A. Billard, "Active teaching in robot programming by demonstration," in *RO-MAN 2007-The 16th IEEE International Symposium on Robot and Human Interactive Communication*. IEEE, 2007, pp. 702–707.
- [5] A. Billard, S. Calinon, R. Dillmann, and S. Schaal, "Survey: Robot programming by demonstration," Springer, Tech. Rep., 2008.
- [6] A. J. Ijspeert, J. Nakanishi, H. Hoffmann, P. Pastor, and S. Schaal, "Dynamical movement primitives: learning attractor models for motor behaviors," *Neural computation*, vol. 25, no. 2, pp. 328–373, 2013.
- [7] B. Fang, S. Jia, D. Guo, M. Xu, S. Wen, and F. Sun, "Survey of imitation learning for robotic manipulation," *International Journal of Intelligent Robotics and Applications*, vol. 3, pp. 362–369, 2019.
- [8] N. Hogan and D. Sternad, "Dynamic primitives of motor behavior," *Biological cybernetics*, vol. 106, no. 11, pp. 727–739, 2012.
- [9] —, "Dynamic primitives in the control of locomotion," *Frontiers in computational neuroscience*, vol. 7, p. 71, 2013.
- [10] N. Hogan, "Physical interaction via dynamic primitives," in *Geometric and numerical foundations of movements*. Springer, 2017, pp. 269–299.
- [11] N. Hogan and S. P. Buerger, "Impedance and interaction control," in *Robotics and automation handbook*. CRC press, 2018, pp. 375–398.
- [12] C. S. Sherrington, *The integrative action of the nervous system*. A. Constable, 1906.
- [13] N. A. Bernstein, "The problem of interrelation between coordination and localization," *Arch Biol Sci*, vol. 38, pp. 1–35, 1935.
- [14] P. Morasso, "Spatial control of arm movements," *Experimental brain research*, vol. 42, no. 2, pp. 223–227, 1981.
- [15] T. Flash and B. Hochner, "Motor primitives in vertebrates and invertebrates," *Current opinion in neurobiology*, vol. 15, no. 6, pp. 660–666, 2005.
- [16] E. Bizzi and F. A. Mussa-Ivaldi, "The acquisition of motor behavior," in *The brain*. Routledge, 2017, pp. 217–232.
- [17] A. d'Avella, P. Saltiel, and E. Bizzi, "Combinations of muscle synergies in the construction of a natural motor behavior," *Nature neuroscience*, vol. 6, no. 3, pp. 300–308, 2003.
- [18] A. d'Avella, "Modularity for motor control and motor learning," *Progress in Motor Control: Theories and Translations*, pp. 3–19, 2016.
- [19] M. L. Latash, "One more time about motor (and non-motor) synergies," *Experimental Brain Research*, vol. 239, no. 10, pp. 2951–2967, 2021.
- [20] S. Schaal, "Dynamic movement primitives—a framework for motor control in humans and humanoid robotics," in *Adaptive motion of animals and machines*. Springer, 2006, pp. 261–280.
- [21] N. Hogan, "Contact and physical interaction," *Annual Review of Control, Robotics, and Autonomous Systems*, vol. 5, pp. 179–203, 2022.
- [22] —, "Impedance control: An approach to manipulation," in *1984 American control conference*. IEEE, 1984, pp. 304–313.
- [23] —, "Impedance control—an approach to manipulation. i-theory. ii-implementation. iii-applications," *ASME Journal of Dynamic Systems and Measurement Control B*, vol. 107, pp. 1–24, 1985.
- [24] —, "Stable execution of contact tasks using impedance control," in *Proceedings. 1987 IEEE International Conference on Robotics and Automation*, vol. 4. IEEE, 1987, pp. 1047–1054.
- [25] N. Hogan and D. Sternad, "On rhythmic and discrete movements: reflections, definitions and implications for motor control," *Experimental brain research*, vol. 181, no. 1, pp. 13–30, 2007.
- [26] J. R. Andrews and N. Hogan, "Impedance control as a framework for implementing obstacle avoidance in a manipulator," Master's thesis, M. I. T., Dept. of Mechanical Engineering, 1983.
- [27] W. S. Newman, "High-speed robot control in complex environments," Ph.D. dissertation, Massachusetts Institute of Technology, 1987.
- [28] J. Hermus, J. Lachner, D. Verdi, and N. Hogan, "Exploiting redundancy to facilitate physical interaction," *IEEE Transactions on Robotics*, vol. 38, no. 1, pp. 599–615, 2021.
- [29] S. Hjorth, J. Lachner, S. Stramigioli, O. Madsen, and D. Chrysostomou, "An energy-based approach for the integration of collaborative redundant robots in restricted work environments," in *2020 IEEE/RSJ International Conference on Intelligent Robots and Systems (IROS)*. IEEE, 2020, pp. 7152–7158.
- [30] A. Ude, B. Nemeč, T. Petrić, and J. Morimoto, "Orientation in cartesian space dynamic movement primitives," in *2014 IEEE International Conference on Robotics and Automation (ICRA)*. IEEE, 2014, pp. 2997–3004.
- [31] M. Saveriano, F. Franzel, and D. Lee, "Merging position and orientation motion primitives," in *2019 International Conference on Robotics and Automation (ICRA)*. IEEE, 2019, pp. 7041–7047.
- [32] C. G. Atkeson, A. W. Moore, and S. Schaal, "Locally weighted learning," *Lazy learning*, pp. 11–73, 1997.
- [33] S. Schaal and C. G. Atkeson, "Constructive incremental learning from only local information," *Neural computation*, vol. 10, no. 8, pp. 2047–2084, 1998.
- [34] P. Pastor, H. Hoffmann, T. Asfour, and S. Schaal, "Learning and generalization of motor skills by learning from demonstration," in *2009 IEEE International Conference on Robotics and Automation*. IEEE, 2009, pp. 763–768.
- [35] P. Pastor, L. Righetti, M. Kalakrishnan, and S. Schaal, "Online movement adaptation based on previous sensor experiences," in *2011 IEEE/RSJ International Conference on Intelligent Robots and Systems*. IEEE, 2011, pp. 365–371.
- [36] P. Pastor, M. Kalakrishnan, F. Meier, F. Stulp, J. Buchli, E. Theodorou, and S. Schaal, "From dynamic movement primitives to associative skill memories," *Robotics and Autonomous Systems*, vol. 61, no. 4, pp. 351–361, 2013.
- [37] F. J. Abu-Dakka, B. Nemeč, J. A. Jørgensen, T. R. Savarimuthu, N. Krüger, and A. Ude, "Adaptation of manipulation skills in physical contact with the environment to reference force profiles," *Autonomous Robots*, vol. 39, pp. 199–217, 2015.
- [38] R. M. Murray, S. S. Sastry, and L. Zexiang, "A mathematical introduction to robotic manipulation," 1994.
- [39] K. M. Lynch and F. C. Park, *Modern robotics*. Cambridge University Press, 2017.
- [40] M. Takegaki, "A new feedback method for dynamic control of manipulators," *Trans. ASME, Ser. G, J. Dynamic Systems, Measurement, and Control*, vol. 103, no. 2, pp. 119–125, 1981.
- [41] J.-J. E. Slotine, W. Li *et al.*, *Applied nonlinear control*. Prentice hall Englewood Cliffs, NJ, 1991.
- [42] S. Arimoto, M. Sekimoto, H. Hashiguchi, and R. Ozawa, "Natural resolution of ill-posedness of inverse kinematics for redundant robots: A challenge to bernstein's degrees-of-freedom problem," *Advanced Robotics*, vol. 19, no. 4, pp. 401–434, 2005.
- [43] S. Arimoto and M. Sekimoto, "Human-like movements of robotic arms with redundant dofs: virtual spring-damper hypothesis to tackle the bernstein problem," in *Proceedings 2006 IEEE International Conference on Robotics and Automation, 2006. ICRA 2006*. IEEE, 2006, pp. 1860–1866.
- [44] F. Caccavale, B. Siciliano, and L. Villani, "Quaternion-based impedance with nondiagonal stiffness for robot manipulators," in *Proceedings of the 1998 American Control Conference. ACC (IEEE Cat. No. 98CH36207)*, vol. 1. IEEE, 1998, pp. 468–472.
- [45] J. Lachner, "A geometric approach to robotic manipulation in physical human-robot interaction," Ph.D. dissertation, University of Twente, 2022.
- [46] N. Hogan and T. Flash, "Moving gracefully: quantitative theories of motor coordination," *Trends in neurosciences*, vol. 10, no. 4, pp. 170–174, 1987.
- [47] B. Nemeč and A. Ude, "Action sequencing using dynamic movement primitives," *Robotica*, vol. 30, no. 5, pp. 837–846, 2012.
- [48] S. Degallier, C. P. Santos, L. Righetti, and A. Ijspeert, "Movement generation using dynamical systems: a humanoid robot performing a drumming task," in *2006 6th IEEE-RAS International Conference on Humanoid Robots*. IEEE, 2006, pp. 512–517.
- [49] S. Degallier, L. Righetti, and A. Ijspeert, "Hand placement during quadruped locomotion in a humanoid robot: A dynamical system approach," in *2007 IEEE/RSJ International Conference on Intelligent Robots and Systems*. IEEE, 2007, pp. 2047–2052.
- [50] S. Degallier, L. Righetti, L. Natale, F. Nori, G. Metta, and A. Ijspeert, "A modular bio-inspired architecture for movement generation for the infant-like robot icub," in *2008 2nd IEEE RAS & EMBS International*

Conference on Biomedical Robotics and Biomechatronics. IEEE, 2008, pp. 795–800.

- [51] J. Buchli, F. Stulp, E. Theodorou, and S. Schaal, “Learning variable impedance control,” *The International Journal of Robotics Research*, vol. 30, no. 7, pp. 820–833, 2011.